

# HENRY

Hydraulic Engineering Repository

Ein Service der Bundesanstalt für Wasserbau

---

Conference Paper, Published Version

**Li, Honghai; Lin, Lihwa; Cho, Kwangwoo**

## **Coastal Inundation from Sea Level Rise and Typhoon Maemi**

Zur Verfügung gestellt in Kooperation mit/Provided in Cooperation with:  
**Kuratorium für Forschung im Küsteningenieurwesen (KFKI)**

---

Verfügbar unter/Available at: <https://hdl.handle.net/20.500.11970/108461>

Vorgeschlagene Zitierweise/Suggested citation:

Li, Honghai; Lin, Lihwa; Cho, Kwangwoo (2016): Coastal Inundation from Sea Level Rise and Typhoon Maemi. In: Yu, Pao-Shan; Lo, Wie-Cheng (Hg.): ICHE 2016. Proceedings of the 12th International Conference on Hydroscience & Engineering, November 6-10, 2016, Tainan, Taiwan. Tainan: NCKU.

### **Standardnutzungsbedingungen/Terms of Use:**

Die Dokumente in HENRY stehen unter der Creative Commons Lizenz CC BY 4.0, sofern keine abweichenden Nutzungsbedingungen getroffen wurden. Damit ist sowohl die kommerzielle Nutzung als auch das Teilen, die Weiterbearbeitung und Speicherung erlaubt. Das Verwenden und das Bearbeiten stehen unter der Bedingung der Namensnennung. Im Einzelfall kann eine restriktivere Lizenz gelten; dann gelten abweichend von den obigen Nutzungsbedingungen die in der dort genannten Lizenz gewährten Nutzungsrechte.

Documents in HENRY are made available under the Creative Commons License CC BY 4.0, if no other license is applicable. Under CC BY 4.0 commercial use and sharing, remixing, transforming, and building upon the material of the work is permitted. In some cases a different, more restrictive license may apply; if applicable the terms of the restrictive license will be binding.

Verwertungsrechte: Alle Rechte vorbehalten

## Coastal Inundation From Sea Level Rise and Typhoon Maemi

*Honghai Li<sup>1</sup>, Lihwa Lin<sup>1</sup>, Kwangwoo Cho<sup>2</sup>*

1. Coastal Engineering Branch, Coastal & Hydraulics Laboratory  
Vicksburg, Mississippi, USA
2. Korea Environment Institute  
Sejong, Korea

### ABSTRACT

Climate change and increasing relative sea level threaten vulnerable coastal communities. The Coastal Modeling System (CMS) was applied to simulate coastal inundation with design SLR scenarios during the passage of Typhoon Maemi and to understand the effects of sea level rise and coastal storms on changes in City of Masan and natural systems. The maximum surge level would reach to 2.3 m under the existing condition. Associated with storm surge and SLR, extensive inundation occurs at Masan.

**KEY WORDS:** Coastal inundation; hydrodynamics; numerical modeling, sea level rise; storm surge; Typhoon Maemi.

### INTRODUCTION

Based on long-term data and observations, increasing atmospheric concentrations of greenhouse gases are warming the atmosphere and the oceans at an accelerated rate (IPCC 2014, Parris et al. 2012). The global warming and the rise in ocean temperature result in an increase of ocean volume and a change in sea level. Global sea level rise (SLR), combined with coastal storms, will cause increased damage to coastal infrastructures, beach erosion and shoreline recess, saltwater intrusion into aquifers and surface waters, rising water tables, and changes in tidal prism (Church et al. 2010). Recognizing climate change with sea level rise threats, the measures needs to be taken to assess vulnerability of coastal communities, to develop technologies to conduct quantitative risk assessment, and to make sound decisions regarding threats to existing and future coastal development.

In this study, ERDC-CHL and Korea Environment Institute (KEI) will identify and utilize the advantage of the vulnerability assessment model, and develop plans to assess vulnerability of coastal communities and to develop technologies for quantitative risk assessment of coastal infrastructure. As the first step of the effort, the pilot study will be conducted at Masan, Korea (Fig. 1), where a coastal modeling system will be developed. The risk assessment study with quantitative modeling technology is developed to understand the effects of sea level rise and coastal storms on changes in both the selected site and natural systems (Burks-Copes et al., 2014).

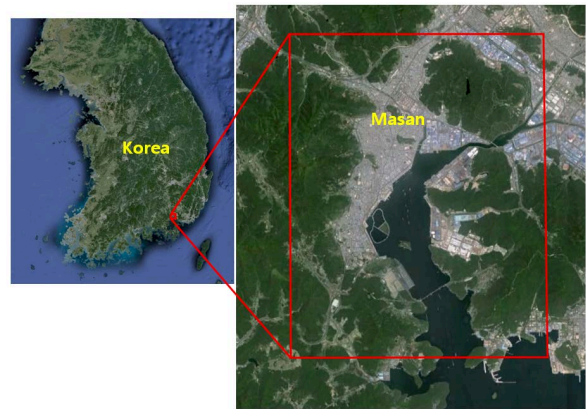


Fig. 1 Masan, Korea. The red rectangular indicates the CMS modeling domain.

### METHOD

#### Model

The Coastal Modeling System (CMS) is used to capture nearshore effects of coastal storms combined with SLR in this study. The CMS is an integrated suite of numerical models for simulating water surface elevation, current, waves, and sediment transport for coastal and inlet applications. The CMS consists of a hydrodynamic and sediment transport model, CMS-Flow, and a spectral wave transformation model, CMS-Wave.

CMS-Flow is a two-dimensional (2D) finite-volume model that solves the mass conservation and shallow-water momentum equations of water motion on a non-uniform Cartesian grid or a telescoping grid. (Sanchez et al. 2011).

CMS-Wave is a 2D spectral wave transformation model that solves the steady-state wave-action balance and diffraction equation on a non-uniform Cartesian grid (Lin et al. 2011). The model simulates important wave processes at coastal inlets including diffraction, refraction, reflection, wave breaking and dissipation mechanisms, wave-wave and wave-current interactions, and wave generation and growth.

CMS-Flow is forced by offshore water surface elevation (typically from tide and storm surge), wind, waves, and river discharge. CMS-Wave is driven by wave spectra and wind, which are often obtained from offshore ocean buoys. During Typhoon Maemi, the sea level rise scenarios are prescribed as 0 (existing condition), 0.5, and 1 m. The CMS capability for nearshore surge calculations was demonstrated with measurements from Typhoon Maemi. The CMS was set up to simulate Typhoon Maemi for the period from 11-15 September, 2003.

### Model Domain

A CMS domain is established surrounding Masan (Fig. 2). The model domain, covering the city and the bay area, extends approximately 8 km from east to west and 12 km from north to south. The southern open boundary is located at the mouth of the bay. In this application, a telescoping grid system with more than 250,000 grid cells is created to discretize the entire city and the nearshore region. The grid system permitted much finer resolution (10 m) in areas of high interest such as the city of Masan. The mesh of the regional model will be coupled with the CMS through data mapping.

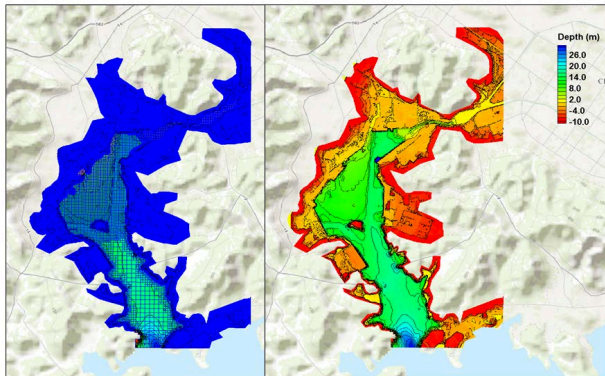


Fig. 2 The Masan model domain and telescoping grid, and water depth and land surface topography contours (relative to MSL).

Coastline information is extracted from the aerial photographs from Google Earth Pro 5.1 (<http://earth.google.com>, accessed 15 September 2014) (Fig. 1). Topographic information of land areas and bathymetry for the water domain are provided by a 5-m resolution coastal digital elevation model (DEM) of Masan. Fig. 2 also shows water depth and land surface topography contours (relative to the WGS84 datum) from the dataset. The figure displays the deep bay area with an average water depth of 11.0 m. The data ranges from the highest elevation of about 10 m on land (negative values) to 30 m at the entrance of the bay (positive values).

The CMS-Wave modeling was performed on a nested grid system with a parent grid covering the regional coastal region and a child grid covering the entire Masan Bay (Fig. 3). The parent grid domain covers an area of approximately 58 x 62 km. It consists of 239 x 246 cells with constant cell spacing of 250 m. The bathymetry data were based on Digital Nautical Chart (DNC) by the US National Geospatial Intelligence Agency (<http://msi.nga.mil/NGAPortal/DNC.portal>, accessed 20 November 2014). The child grid covers the same area as the Masan Bay flow model domain, a rectangular area of approximately 8.5 x 12 km. The child grid consists of 850 x 1185 cells with a constant cell spacing of 10 m. The orange zone corresponds to the area with the ground elevation between 0 and 5 m (WGS84).

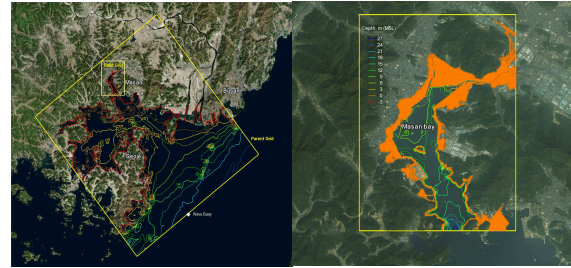


Fig. 3 CMS-Wave parent and child rectangular grid domains with bathymetry contours and with potential flooding area (orange zone).

### Model Input

Tide, surge, wind, and waves will serve as physical forcing input to the nearshore modeling. Surge information is retrieved from a large scale regional model output, Advanced CIRCulation model (ADCIRC) (Luettrich and Westerink 2004), and tide data are obtained from the tidal gauge. The combination of the two datasets provides the water surface elevation forcing along the CMS open boundaries.

Wind and wave data are provided at a tidal gauge and an ocean buoy near Masan, Korea (Fig. 4). The 2012 wind speed and direction, and wave parameters were measured at the moored buoy (GEOJEDO) offshore Busan, which indicate that two strong storm events occurred in late August and mid-September. Peak wind speeds are greater than 20 m/sec during the storms. Storm waves propagated from west-northwest with wave periods of 13 sec and significant wave heights greater than 6 m. Local wind is much weaker due to land sheltering effect. Hourly water surface elevations show a tidal range of about 2 m.

### TYPHOON MAEMI

Category 5 super Typhoon Maemi occurred in 5-13 September, 2003. Maemi formed initially from a disturbance in the west central Pacific Ocean. It intensified to a typhoon on 8 September and became Category 5 on 10 September while passed over the Japanese island of Miyako-Jima. It made landfall west of Busan, South Korea, as a Category 3 cyclone on 12 September. The typhoon became extra-tropical in the Sea of Japan the next day and remnants persisted for several days lashing northern Japan with strong winds. Damage was heaviest with extensive coastal flooding and wind damage to properties in the southern Korea Peninsula, particularly where it moved ashore (Yasuda et al. 2005).

The CMS was set up to simulate Typhoon Maemi for the period from 11-15 September, 2003. Each simulation is designed to run over a four-day duration to cover a 12-hour ramping of transition from normal to storm condition, and the passage of the storm. Specifications of the primary driving forces for Typhoon Maemi are described as follows.

### Water Surface Elevation

Astronomical tide and storm surge were measured at Masan gauge (Fig. 4) and specified along the CMS open boundary at the bay entrance (Fig. 2). Fig. 5 shows the input water surface elevation data during the 5-day simulation period (11-15 September 2003). The time series data displays that Typhoon Maemi made landfall during spring tide and the maximum surge level reached 4.2 m above the WGS84 datum, which is 2 m higher than mean high water spring tidal level.



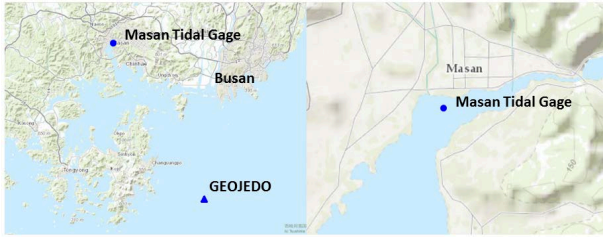


Fig. 4 Location of Masan tidal gauge and GEOJEDO buoy.

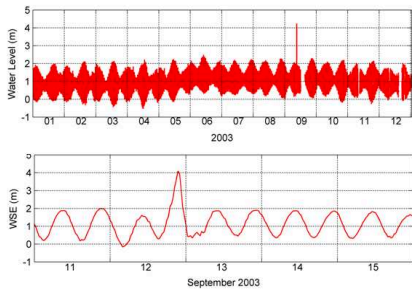


Fig. 5 The 2003 water level measured at the Masan tidal gauge.

### Wind and Waves

Wind and waves were measured from the GEOJEDO buoy. Fig. 6 shows the wind speed and direction for 11-15 September, 2003. The maximum wind speed was approximately 27 m/sec and the change in wind direction from east to south southwest indicates the typhoon passage. The time series of wave parameters indicate that incident storm waves propagated from the East China Sea through Korea Strait with a wave period of 16.7 sec and a peak wave height of 7 m.

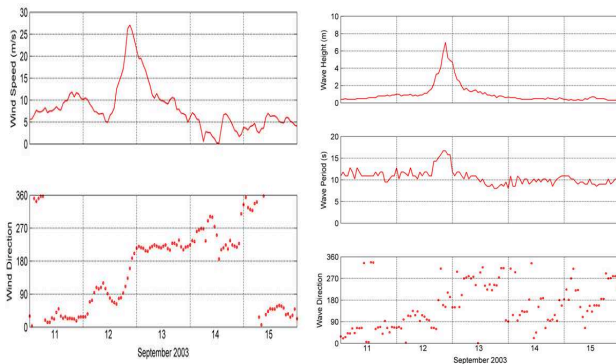


Fig. 6 Wind speed and direction, and wave parameters measured at the GEOJEDO buoy during Typhoon Maemi.

### Wave Model Forcing and Specifications

CMS-Wave is normally forced by either incident waves specified along the seaward boundary or atmospheric wind input applied to the model domain or both. In the present grid system, the parent grid is forced by incident waves provided at the southeast boundary (Korean Strait) and wind input over the parent grid domain. Both incident waves and wind input over the parent grid domain. Both incident waves and wind input information are based on the hourly data collected from the GEOJEDO buoy. For the child grid, CMS-Wave is coupled with CMS-Flow with incident waves computed from the parent grid along the south boundary (lower Masan Bay) of the child grid. Wave run-up is

calculated in the child grid in the area with the ground elevation between 0 and 5 m (WGS84). It contributes to water level rise and provides wave stresses to increase the flow rushing up the shore and overtopping structures.

### RESULTS

CMS-Flow and CMS-Wave were dynamically coupled during the simulation at a 1-hour interval. The coupling process was repeated for the 5-day duration of the Typhoon Maemi simulation.

Fig. 7 shows the location of three selected sites in Masan Bay and the hourly water surface elevation at those sites. The maximum typhoon-induced surge occurred on 12 September, 2003 at 22:00 LST. Corresponding to the typhoon passage, water pileup against coast is displayed by the maximum surge values of 4.1, 4.4 and 4.5 m (WGS84) at Lower Bay, Masan, and Upper Bay, respectively.

Current fields during the typhoon passage (12 September at 20:00 to 13 September at 02:00) are analyzed. The flow pattern in the bay clearly corresponds to the typhoon passage. The current speed is between 0.2 and 0.4 m/sec in the lower and middle bay, and can be as high as 0.8 m/sec in the upper bay with a narrow waterway.

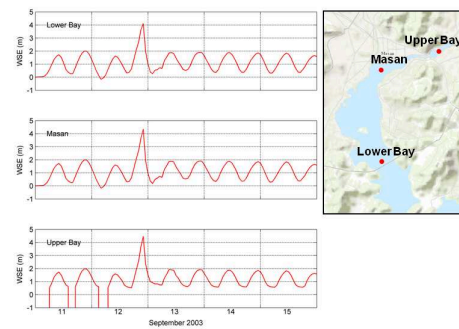


Fig. 7 Location of three selected sites in Masan Bay and the hourly water surface elevation at those sites.

Fig. 8 shows the calculated maximum wave height fields corresponding to strong surface wind on 12 September, 2003 at 21:00 LST in the parent and child grids, respectively. The incident wave height specified at the seaward boundary of the parent grid is approximately 7 m. At the same time, the incident waves enter the lower Masan Bay at the child grid south boundary is approximately 1m as calculated from the parent grid. With strong wind and extreme storm surge, the calculated maximum wave height reaches to 0.8 m along the northwest perimeter of Masan Bay.

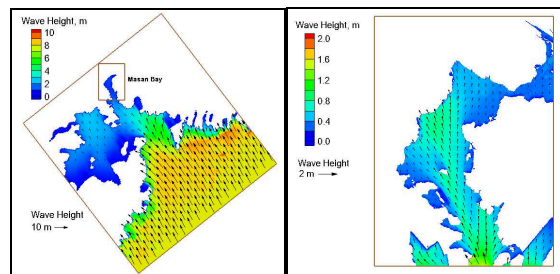


Fig. 8 Calculated wave fields in the parent and the child grid on 12 September 2003 at 21:00 LST.

To assess the land inundation, a land area is defined based on the Google map. The area is shown in Fig. 9 with a maroon line polygon, within which the land elevation varies from the zero mean sea level to 10 m above the WGS84 datum. Fig. 9 also shows the spatial distribution of the water surface elevations on 12 September, 2003 at 22:00 LST. The color shaded area within the polygon indicates the flooded land area along the shoreline in Masan Bay. The results show that about 30% of the defined polygon area around Masan was inundated from Typhoon Maemi. The flooded harbor area is generally flat and has a ground elevation of about 2.5-3 m above WGS84, and the other areas have a ground elevation of less than 4.5 m above WGS84. Because waves break in shallow water, the CMS-calculated significant wave heights at the flooded higher ground have a small averaged value of 20 cm.

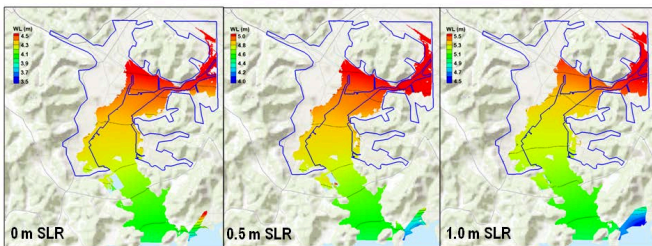


Fig. 9 The spatial distribution of the water surface elevations on 12 September, 2003 at 22:00 LST. The blue line polygon delineates the land area around Masan, within which the land elevation varies from the zero mean sea level to 10 m above the WGS84 datum.

The maximum surge level induced by Typhoon Maemi would reach to 2.3 m under the existing condition (0 m sea level rise). Associated with the storm surge and sea level rises, extensive inundation occurs at Masan. Corresponding to the 0.5 m and 1 m SLR scenarios during Typhoon Maemi, the extreme water level could inundate approximately 30-35% of the Masan area defined in this study.

## CONCLUSIONS

In this pilot study, oceanic and atmospheric data were assembled around Masan and CMS input was prepared. Based on the available data, flow and wave simulations were conducted for Typhoon Maemi. The model results show that the maximum surge was 4.5 m (WGS84), 2 m above the mean high water, and the maximum vertically averaged current speed was 0.8 m/sec in the upper Masan Bay during the passage of Typhoon Maemi. The calculated maximum wave height reaches to 0.8 m along the northwest perimeter of Masan Bay. Based on the model calculations, the flooding map was generated in Masan Bay. Approximately 30% of the land area defined around Masan was inundated from Typhoon Maemi.

The CMS was used to evaluate coastal inundation caused by storm surge, waves, and wind. The accuracy of the model results is determined by the calculated water surface elevations and the measurements of land surface topography. Land inundation maps will provide assistance to coastal vulnerability and risk assessment, and need to be updated with designed sea level rise scenarios.

## ACKNOWLEDGEMENTS

The authors wish to thank for the support of "Cooperative Research Program for Agriculture Science & Technology Development Project No. PJ010475012016", Rural Development Administration, Republic of Korea, and the US Army Engineer Research & Development Center, Coastal Inlets Research Program. Permission was granted by the Chief, US Army Corps of Engineers to publish this information.

## REFERENCES

- Burks-Copes, K. A., and Russo, E. J. (2014). Risk Quantification for Sustaining Coastal Military Installation Assets and Mission Capabilities, Final Technical Report. Prepared by the U.S. Army Engineer Research and Development Center (ERDC), Environmental Laboratory (EL), Vicksburg, MS for the Strategic Environmental Research and Development Program (SERDP) under project #RC-1701.
- Church, J. A., Aarup, T., Woodworth, P. L., Wilson, W. S., Nicholls, R. J., Rayner, R., Lambeck, K., Mitchum, G. T., Steffen, K., Cazenave, A., Blewitt, G., Mitrovica, J. X., and Lowe, J. A. (2010). Sea level rise variability - synthesis and outlook for the future (Chapter 13). In, *Understanding Sea Level Rise and Variability* by Church, J. A., P. L. Woodworth, T. Aarup, and W. S. Wilson (eds.), Wiley-Blackwell.
- Intergovernmental Panel on Climate Change (IPCC) (2014). Fifth assessment report. Available online at: <http://www.ipcc.ch/> (Accessed 10 March 2014).
- Lin, L., Demirebilek, Z., Thomas, R., and Rosati III, J. (2011). Verification and Validation of the Coastal Modeling System, Report 2: CMS-Wave. Coastal and Hydraulics Laboratory Technical Report ERDC/CHL-TR-11-10. Vicksburg, MS: US Army Engineer Research and Development Center.
- Luetlich, R. A. and Westerink, J.J. (2004). Formulation and Numerical Implementation of the 2D/3D ADCIRC Finite Element Model Version 44. [adcirc.org](http://adcirc.org/adcirc_theory_2004_12_08.pdf). Available online at: [http://adcirc.org/adcirc\\_theory\\_2004\\_12\\_08.pdf](http://adcirc.org/adcirc_theory_2004_12_08.pdf) (Accessed 23 Feb. 2012).
- Parris, A., Bromirski, P., Burkett, V., Cayan, D., Culver, M., Hall, J., Horton, R., Knutti, K., Moss, R., Obeysekera, J., Sallenger, A., and Weiss, J. (2012). *Global Sea Level Rise Scenarios for the U.S. National Climate Assessment*. NOAA Tech Memo OAR CPO-1. 37 pp.
- Sanchez, A., Wu, W., Beck, T. W., Li, H., Rosati III, J., Thomas, R., Rosati, J. D., Demirebilek, Z., Brown, M., and Reed, C. W. (2011). Verification and validation of the Coastal Modeling System, Report 3: Hydrodynamics. Coastal and Hydraulics Laboratory Technical Report ERDC/CHL-TR-11-10. Vicksburg, MS: U. S. Army Engineer Research and Development Center.
- Yasuda, T., Hiraishi, T., Kawai, H., Nagase, K., Kang, S. W., and Jeong, W. M. (2005). Field survey and computation analysis of storm surge disaster in Masan due to Typhoon Maemi. *Proceeding of Asian and Pacific Coasts*, 4-8 September, 2005, Jeju, Korea.